BLIND IDENTIFICATION OF QAM SIGNALS USING A LIKELIHOOD-BASED ALGORITHM

Daimei Zhu, V. John Mathews

University of Utah
Department of Electrical and Computer Engineering
Salt Lake City, Utah 84112
Email: daimei.zhu@utah.edu (D. Zhu)
mathews@ece.utah.edu (V. J. Mathews)

ABSTRACT

This paper presents a method for automatically identifying different QAM modulations. This method identifies the modulation type as the hypothesis for which the likelihood function of the amplitudes of the received signal is the maximum. The derivation of the likelihood functions assumes additive white Gaussian noise and no pulse shaping. In order to accommodate pulse shaping in the received signal, the system sub-samples the incoming signals non-uniformly so that the distribution of the amplitudes of the sub-sampled signals approximately matches that of QAM signals without pulse shaping. This method does not need prior knowledge of carrier frequency and baud rate and can identify modulation types at relatively low SNRs and with relatively few symbols. Simulation results demonstrating accurate modulation identification in the presence of additive noise are included in the paper. Results presented in the paper with non-Gaussian noise indicate that the system is robust to variations from the assumed noise model.

Index Terms— Blind Modulation identification, likelihood function, QAM signal

1. INTRODUCTION

Automatic identification of the modulation type of a received signal is important in many military and civil applications. Blind modulation identification, *i. e.*, modulation identification without *a priori* knowledge of the carrier frequency, symbol rate and other parameters of signal transmission, is addressed in this paper. We assume that the received signal is quadrature-amplitude-modulated, but do not assume any prior knowledge of the order of QAM modulation.

In [1], the authors proposed a method for QAM modulation identification based on computation of the likelihood function of the signal amplitudes. This approach does not need prior knowledge of the carrier frequency and symbol rate. However, the authors do not take pulse shaping of the symbols into consideration in their signal models, and direct application of the method on pulse shaped signals results in poor performance. A different approach to QAM modulation identification that employed cyclic cumulants of the received signals was described in [2]. This method requires knowledge of the symbol rate and the carrier frequency for good performance. A clustering-based distribution fitting algorithm is used for modulation identification in [3], but the results presented in the paper indicate that the method needs input signals with relatively high signal-to-noise ratios to accurately identify QAM and PSK signals.

In this paper, we consider likelihood-based identification of QAM modulation types including PSK, 16QAM, 32QAM, etc. without *a priori* knowledge of symbol rate, carrier frequency and noise power. Our method differs from methods available in the literature in two significant ways: (1) we modify the likelihood-based method for the amplitudes derived in [1] to accommodate received signals with pulse shaping. Our method employs "matched filtering" and non-uniform subsampling process to decrease the effect of pulse shaping on the amplitude and does not require knowledge of the pulse shape; (2) The likelihood function depends on the signal amplitude and the noise power, both of which are unknown. The algorithm presented here finds the maximum likelihood function corresponding to the correct modulation type and the right environmental parameters. This paper only addresses PSK as a special case of QAM modulation. The problem of identifying different PSK modulation types will be addressed elsewhere.

The rest of the paper is organized as follows: the received signal model with pulse shaping is described in the next section. The likelihood-based identification method for signals without pulse shaping is presented in Section 3. An approach to sub-sample the received signals non-uniformly in such a way that the distribution of the amplitude of the sub-sampled signals is approximately the same as that of the amplitude of the signals without pulse shaping is described next. The sub-sampling process utilizes a coarse estimate of the symbol

duration made from the estimated spectrum of the received signal. Section 4 explains the classification between QAM-16 signal and PSK signals. The overall approach for blind modulation identification that combines the techniques of Sections 3 and 3.3 is presented in Section 5. Section 6 contains simulation results demonstrating that the method of this paper is capable of accurate modulation identification with relatively small number of input samples and in relatively low SNR conditions. Finally, Section 7 contains the concluding remarks.

2. SIGNAL MODEL

We assume an additive band limited white Gaussian channel under which the general model for the received signal [6] is

$$y(t) = Re\{\sum_k (s_k g_T(t - kT_b))e^{j2\pi f_c t} + N_0(t)\} \quad (1)$$

where s_k is a complex symbol sequence with $s_k = a_k + jb_k$, where a_k and b_k are, respectively, the real and imaginary parts of the symbol s_k, T_b is the symbol period, $g_T(t)$ is the square-root raised-cosine pulse shape filter with unknown roll-off factor, f_c is the carrier frequency, and N_0 is additive band limited white Gaussian noise. We assume that N_0 is such that the sampled version of the noise is independent identically distributed Gaussian signals with zero mean value and variance σ^2. Applying Hilbert transformation to the received signals, the output will become

$$y(t) = \sum_k (s_k g_T(t - kT_b))e^{j2\pi f_c t} + N_0(t) \quad (2)$$

In our derivations, we use a signal model corresponding to an appropriately sampled version of this signal, as given by

$$y(n) = \sum_k (s_k g_T(nT_s - kT_b))e^{j2\pi f_c nT_s} + N_0(nT_s) \quad (3)$$

where T_s is the sampling period. We assume that the pulse shaping is such that the interference between adjacent symbols is negligible at the mid-point of each baud [5]. Let $y(l)$ represent the mid-point of the lth symbol. Under the above assumption, $y(l)$ can be modeled as

$$y(l) = s_l g_T(0)e^{j2\pi f_c lT_b} + N_0(l) \quad (4)$$

where $N_0(l)$ is the noise sample at the mid-point of the l_{th} symbol. The amplitude of received signal after sub-sampling considering the noise is

$$|y(l)|^2 = |s_l g_T(0)|^2 + n_0(l) \quad (5)$$

where $n_0(l) = 2\Re\{s_l g_T(0)e^{j2\pi f_c lT_b} N_0^*(l)\} + |N_0(l)|^2$ is the component of the received signal amplitude contributed by noise. From the above, we can see that the amplitude of received signals with pulse shaping after sub-sampling as above will have the same distribution (within a scaling factor) as the amplitude of signals without pulse shaping. Since our methods in Section 3 are derived based on pulse shape-free signals, we will introduce in Section 3.3 a method to sub-sample the received signal such that the resulting distribution of the signal amplitude approximately matches that of the pulse shape-free signal.

3. LIKELIHOOD FUNCTION FOR QAM SIGNALS

3.1. Probability Density Function of Signal Amplitudes

For a continuous sinusoid with amplitude S that is perturbed by a white Gaussian noise with variance σ^2 and zero mean value, the probability distribution function (PDF) of its amplitude R is the Rice distribution given by

$$P(R) = \frac{R}{\sigma^2} e^{-(R^2+S^2)/2\sigma^2} I_0(\frac{RS}{\sigma^2}), R \geq 0 \quad (6)$$

where $I_0(\cdot)$ is the zero-order Bessel function of the first kind [7].

For the signal model in Section 2 with no pulse shaping, the amplitude at any time may be thought of as a noisy sinusoid whose amplitude can take one of a finite number of values depending on the modulation order. Furthermore, assuming that the symbols sequence is independent, identically-distributed, the probability of these amplitude values can be pre-determined for each QAM type. Therefore, the distribution of the signal amplitude will be a weighted sum of the Rice distributions corresponding to the different amplitude values.

Let there be N distinct amplitude values for the Mth modulation type. Let the set $\{S_{M,i}; i = 1, 2, \cdots, N\}$ represent these values and let $w_M[i]$ be the probability of the ith amplitude value for the Mth modulation type. The PDF for signal amplitude R will then be

$$\begin{aligned} P(R) &= \sum_{i=1}^{N} (P(R|S_{M,i}) w_M[i])), R \geq 0, \\ &= \sum_{i=1}^{N} w_M[i] \frac{R}{\sigma^2} e^{-(R^2+S_{M,i}^2)/2\sigma^2} I_0(\frac{RS_{M,i}}{\sigma^2}) \end{aligned} \quad (7)$$

In the above equation, $P(R|S_{M,i})$ is the conditional PDF of the signal amplitude given that the modulation type is M.

3.2. Log-likelihood Function-based Classification Algorithm

In this section, we develop a classification method for different QAM signals based on the PDF of their amplitudes. Let H_M represent the hypothesis that the Mth modulation type is the actual modulation type of the received signal. Given n amplitude values $R_1, R_2, \ldots, R_n$ of the received signals, the

conditional probability that H_M is true is given by

$$p(H_M|R_1, R_2, \ldots, R_n) = \frac{p(R_1, R_2, \ldots, R_n|H_M)p(H_M)}{p(R_1, R_2, \ldots, R_n)} \quad (8)$$

where

$$p(R_1, R_2, \ldots, R_n|H_M) = \prod_{i=1}^{n} P(R_i|H_M) \quad (9)$$

Combining (9) with (7), we obtain the conditional probability for the observed amplitude values given the hypothesis of the Mth modulation type as

$$p(R_1, R_2, \ldots, R_n|H_M) = \prod_{i=1}^{n} \left\{ \sum_{i=1}^{N} w_M[i] \frac{R}{\sigma^2} e^{-(R^2+S_{M,i}^2)/2\sigma^2} I_0(\frac{RS_{M,i}}{\sigma^2}) \right\} \quad (10)$$

In this derivation, we assume that the hypotheses for modulation types are equally likely and that $p(R_1, R_2, \ldots, R_n)$ is independent of the hypothesis. As a result, the conditional probability of the hypothesis H_M in (8) is proportional to the conditional probability of the observed amplitudes in (10). In order to simplify the calculations and since natural logarithm is monotonically increasing, we use the natural logarithm of (10) as the decision function for the identification problem. That is, we choose the modulation type that maximizes the log-likelihood function given by

$$l_M = \sum_{i=1}^{n} \ln(\sum_{i=1}^{N} w_M[i] \frac{R}{\sigma^2} e^{\frac{-(R^2+S_{M,i}^2)}{2\sigma^2}} I_0(\frac{RS_{M,i}}{\sigma^2}) \quad (11)$$

3.3. Sub-sampling

We know from our earlier discussion that, under our assumptions, if we sub-sample the received signal at the mid-point of each baud, the amplitude of resulting signal will have similar distribution as that of signal without pulse shaping. In order to be able to sub-sample the received signals, we need to estimate the symbol duration first.

3.3.1. Estimation of the Baud Rate

For this derivation, we assume that a square-root raised-cosine filter with unknown parameter is used for pulse shaping. From the signal model in Section 2, we can show that the spectrum of the received signal is given by

$$S_{xx}(f) = P_s||H(f)||^2 + \sigma^2 \quad (12)$$

where P_s is the clean signal power, $||H(f)||^2$ is the squared magnitude of the frequency response of the pulse shaping filter, and σ^2 is the noise variance. We assume a square-root raised cosine pulse shape for baud rate estimation. Since the squared frequency response of the root-raised cosine filter with parameter β and symbol duration T_b is given by

$$H(f) = \begin{cases} T_b; & |f| \leq \frac{1-\beta}{2T_b} \\ \frac{T_b}{2}\{1 + cos[\frac{\pi T_b}{\beta}(|f| - \frac{1-\beta}{2T_b})]\}; & \frac{1-\beta}{2T_b} \leq |f| \leq \frac{1+\beta}{2T_b} \\ 0; & \text{otherwise} \end{cases} \quad (13)$$

We can estimate the unknown parameters β, T_b and σ^2 from the estimated power spectrum of the received signal. In all our work, the estimation of these parameters were done using least-squares regression after estimating the spectrum using Welch's method [8]. The use of square-root raised-cosine filter model is not critical in this work since only a coarse estimation of the symbol duration is needed.

3.3.2. Filtering the Received Signal

From (12), the frequency response of the square-root raised-cosine filter is the square root of the signal spectrum with a scaling factor. The convolution of two matched square-root raised-cosine filters satisfies Nyquist criterion

$$p(nT_b) = \begin{cases} 1; & n = 0 \\ 0; & \text{otherwise} \end{cases} \quad (14)$$

where $p(t)$ is a Nyquist pulse-shape resulting from the matched filtering operation and T_b is the baud duration. Therefore, we convolve the received signal with the "matched filter" obtained as the inverse Fourier transform of the square root of the estimated spectrum. The signal is

$$\hat{y}(t) = c \sum_{k} (s_k \hat{g}_T(t - kT_b)) e^{j2\pi f_c t} + \hat{N}_0(t) \quad (15)$$

where $\hat{g}_T(t)$ is a Nyquist pulse-shape, c is a constant. The signal in (15) will then satisfy

$$\hat{y}(nT_b) = s[n] + \hat{N}_0(nT_b) \quad (16)$$

3.3.3. Non-uniform Sub-sampling of the Received Signals

The pulse shape filter affects the amplitude distribution of the received signal greatly. Therefore we use sub-sampling to mitigate this effect. Because the estimation of baud rate is not exact, sub-sampling at the mid-point of each baud requires signal interpolation. Our approach attempts to pick the sample that is closest to the mid-point of each baud in the following manner: we start with the sample with the maximum amplitude among samples in the first several symbol durations (4 in the simulation results presented). The sample with the peak value in a small interval in the middle of the next estimated baud of duration $\hat{T}_b/T_s$ samples defined by the samples in the range $[l + \frac{\hat{T}_b}{2T_s}, l + \frac{3\hat{T}_b}{2T_s}]$. For instance, let the

l selected sample be $y(\hat{l})$. That is, the $(l+1)$th sample is selected as

$$\arg\max_{j} \left\{ \hat{y}(\hat{l} + \hat{T}_b/T_s + j)| - r \leq j \leq r \right\} \qquad (17)$$

where we search for the peak over an interval containing $2r$ samples. In all our simulations described in Section 6, we chose r to be the smallest integer larger than or equal to one-fourth of the estimated number of samples per baud. We note that the sub-sampling process described above is non-uniform since the peak values may not be equally spaced from each other.

Figure 1 demonstrates effects of the sub-sampling process. Shown in the figure is one example of the amplitude distribution of received signals before and after sub-sampling for a QAM-16 signal. Parameters for the signals are: SNR = 20 dB; number of symbols $N = 10000$; T_b/T_s = 20. The top left panel shows the scatter plot of the received signal. The histogram of the signal amplitude is shown in the top right panel. The corresponding results after matched filtering and sub-sampling are shown in the bottom panels. The three groups of amplitude of the QAM-16 signals can be observed after matched filtering and sub-sampling, but not in the received signal prior to sub-sampling. Consequently, we can apply the likelihood functions derived for modulation identification of signals without pulse shaping to identify pulse shaped signals after the sub-sampling.

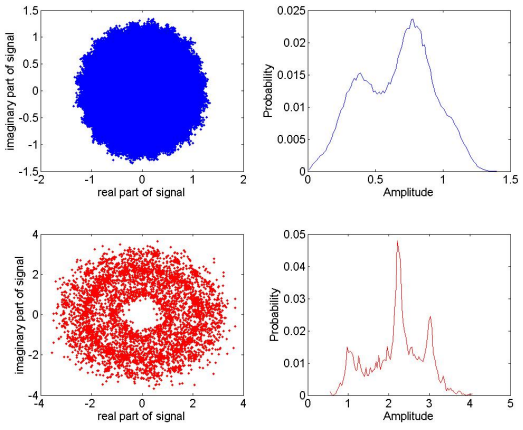

Fig. 1. Scatter plot and amplitude distribution of received signals before and after sub-sampling. Top left: scatter plot of the received QAM-16 signal with pulse shaping; right: histogram of amplitude of the received QAM-16 signal with pulse shaping; bottom left: scatter plot of the QAM-16 signal after matched filtering and sub-sampling; bottom right: histogram of amplitude for QAM-16 signal after matched filtering and sub-sampling.

3.4. Estimation of Unknown Parameters After Sub-sampling

To compute the log-likelihood function in (11), we need to know the symbol amplitudes $S_{M,i}$ and the noise variance σ^2. For a given modulation type, we assume that $S_{M,i}$ is known within a scaling factor. With estimated σ^2, the scaling factor can be easily estimated from the relationship

$$E\{y^2(k)\} = \gamma^2 \sum_{i=1}^{N} w_M[i] S_{M,i}^2 + \sigma^2 \qquad (18)$$

where γ^2 is the scaling factor. Even though we roughly estimated noise power in Section 3.3.1, the error between estimated and real noise power will substantially affect the accuracy of identification. Furthermore, the filtering and sub-sampling process may also change the noise characteristics. In order to improve the accuracy of identification, we use the estimated σ^2 as described earlier in 3.3.1 and search for the σ^2 in a range when $S\hat{N}R - 5dB \leq SNR \leq S\hat{N}R + 5dB$ that maximizes the value of the log-likelihood function (11) for each hypothesis. That is, the modulation identification problem finds the parameter σ^2 and the modulation type M that maximize the log-likelihood function given by

$$\begin{aligned} P_M\left(\gamma^2, \sigma^2\right) = & \quad P\Big(l_M | S\hat{N}R - 5 \leq SNR \leq S\hat{N}R + 5\Big) \\ = & \quad P(\textstyle\sum_{i=1}^{n} \ln(\sum_{i=1}^{N} e^{\frac{-(R^2+\gamma^2 S_{M,i}^2)}{2\sigma^2}} I_0(\frac{R\gamma^2 S_{M,i}}{\sigma^2}) \\ & w_M[i]\tfrac{R}{\sigma^2} | S\hat{N}R - 5 \leq SNR \leq S\hat{N}R + 5) \end{aligned} \qquad (19)$$

4. CLASSIFICATION BETWEEN QAM-16 AND PSK SIGNAL

Even though we only have one amplitude group in PSK symbols, in many situations, the pulse shape filter will add one more prominent amplitude group to the signals. Furthermore, "matched filtering", as described in Section 3.3.2 sometimes introduces a third, prominent amplitude group to the signals, causing the identification system to confuse PSK signals with QAM-16 signals. This problem is occurs mostly with BPSK signals, and is more problematic in high-SNR situations. Figure 2 provides one comparison of the amplitude distribution of PSK signal before and after "matched filtering" and sub-sampling. In order to correctly identify PSK and QAM-16 signals, in such situations, we further analyze signals identified as QAM-16 or PSK. For estimated SNRs above 5 dB, we perform the modulation identification again without the matched filtering and retain the results of this process as the modulation type. We have found this modification to substantially improve the capability of the system to discriminate between PSK and QAM-16 signals.

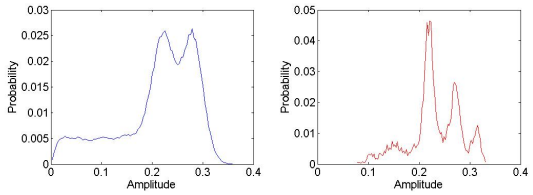

Fig. 2. Amplitude distribution of received signals before and after "matched filtering" and sub-sampling. Left: histogram of amplitude for received BPSK signal with pulse shaping: SNR=20 dB, N=10000; right: histogram of amplitude for BPSK signal after matched filter and sub-sampling.

5. MODULATION IDENTIFICATION STRUCTURE

Figure 3 shows a block diagram of the complete system for the QAM modulation identification. The system first estimates the baud duration as described in Section 3.3, and then filters and sub-samples the received signal. The likelihood function associated with each modulation is then computed. The modulation type that results in the largest value of the likelihood function is selected as the estimated modulation type.

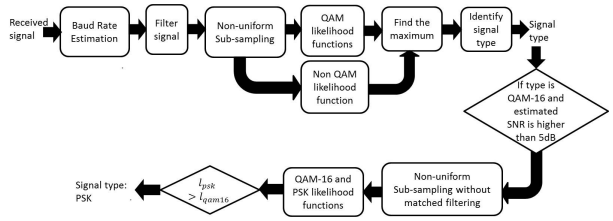

Fig. 3. Block diagram of the modulation identification system.

6. PERFORMANCE EVALUATION

In this section, the performance of the likelihood-based blind modulation identification algorithm is demonstrated by presenting the probability of correctly identifying each modulation type under several SNR conditions. We also provide the performance of the algorithm in noise environments different from the assumed Gaussian model.

6.1. Results for Pulse Shaped Signals in Gaussian noise

Figure 4 shows the probability of correct modulation identification for different SNRs. A root raised cosine filter with parameter $\beta = 0.5$ was applied to the transmitted symbol sequence, and $N = 10000$ symbols were used for the identification. The noise here is zero-mean Gaussian noise. The results demonstrate good performance. For example, the system identified QAM-16 modulation with 100% accuracy at 9 dB SNR. As expected, higher order modulations require higher SNR values for accurate identification.

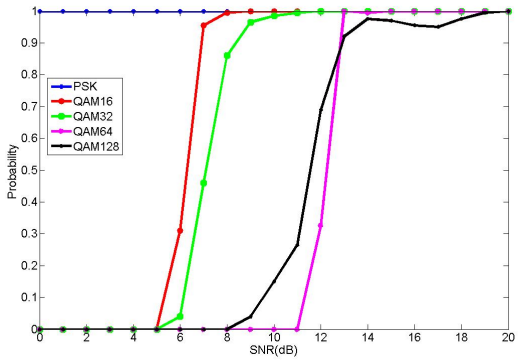

Fig. 4. Probability of correct modulation identification with different SNRs for pulse shaped signals, N=10000.

6.2. Results for Non-Gaussian Noise Environment

Figure 5 and 6 show the probability of correct modulation identification in noise environments different from the assumed Gaussian noise model. The noise in Figure 5 was a zero-mean uniform distribution noise and that resulting in Figure 6 is the Laplacian distribution with zero mean. We observe that uniform noise and Laplacian noise were comparable to the performance in Gaussian noise.

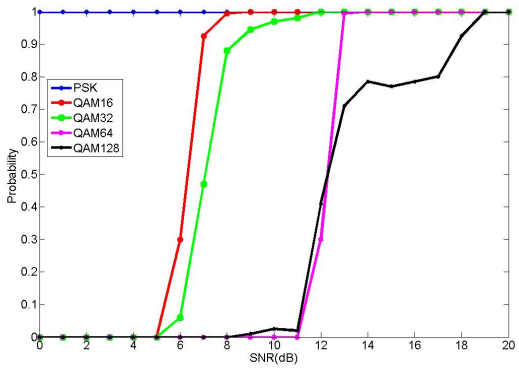

Fig. 5. Probability of correct modulation identification with different SNRs for pulse shaped signals with uniform distribution noise, N=10000.

7. CONCLUSION REMARKS

The likelihood-based modulation identification algorithm presented in this paper appears to have the potential to perform well at relatively low SNRs and using relatively short signal durations. The simulation results presented indicate

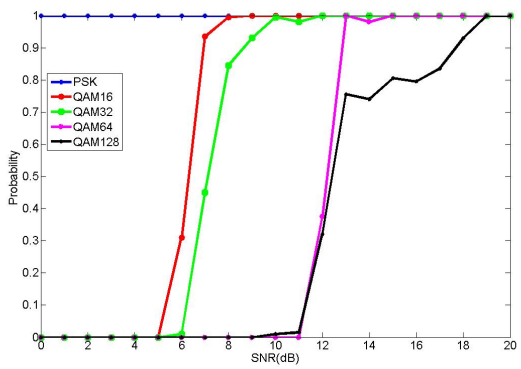

Fig. 6. Probability of correct modulation identification with different SNRs for pulse shaped signals with Laplacian distribution noise, N=10000.

that the performance degradation that comes with pulse shaping is not substantial and the algorithm is robust under different noise environments. Further work on performance evaluation under a variety of impairments as well as algorithm refinements to reduce computational complexity and to improve performance is underway at this time.

Acknowledgment

The work done at the University of Utah was supported in part by a research contract with Raytheon Applied Signal Technology. The authors thank David Detienne for his insights on modulation identification problems, and his valuable help in this research.

8. REFERENCES

[1] Y. Yang, C.-H. Liu, and T.-W. Soong, "A log-likelihood function-based algorithm for QAM signal classification," *Signal Processing*, vol. 70, No. 1, pp. 61-71, Oct. 1998

[2] O. A. Dobre, Y. Bar-Ness, and W. Su, "Robust QAM modulation classification algorithm using cyclic cumulants," *Proc. IEEE Wireless Communications and Networking Conference*, vol. 2, pp. 745-748, Atlanta, USA, 2004.

[3] K.-T. Woo and C.-W. Kok, "Clustering based distribution fitting algorithm for Automatic Modulation Recoginition," *Proc. IEEE Symposium on Computers and Communications*, pp. 13-18, Averio, Portugal, July 2007.

[4] G. Wan, J. Liang, Y. Li and Q.Wu, "An Improved Estimation Algorithm of Symbol Synchronization for QAM Signal," *International Conference on Innovation Management*, pp. 67-70, Wuhan, China, Dec. 2009.

[5] J. Xi and Z. Wang, "MQAM modulation scheme recognition using Hilbert transform," *Journal on Communications*, vol. 28, No. 6, June 2007.

[6] B. Farhang-Boroujeny, *Signal Processing Techniques for Software Radios*, LuLu Publishing House, 2010.

[7] S. O. Rice , "Mathematical analysis of random noise", *Bell System Technical Journal*, vol. 24, No. 1, pp. 46-156, Jan. 1945.

[8] P. D. Welch, "The Use of Fast Fourier Transform for the Estimation of Power Spectra: A Method Based on Time Averaging Over Short, Modified Periodograms," *IEEE Transactions on Audio Electroacoustics*, vol. AU-15, No.2, pp. 70-73, June 1967.